ELSEVIER

Biochimica et Biophysica Acta 1587 (2002) 107–117

BIOCHIMICA ET BIOPHYSICA ACTA
BBA

www.bba-direct.com

Review

Development of transition state analogues of purine nucleoside phosphorylase as anti-T-cell agents

Vern L. Schramm*

Department of Biochemistry, Albert Einstein College of Medicine, 1300 Morris Park Avenue, Forch. 308, Bronx, NY 10461, USA

Received 24 January 2002; accepted 24 January 2002

Abstract

Newborns with a genetic deficiency of purine nucleoside phosphorylase (PNP) are normal, but exhibit a specific T-cell immunodeficiency during the first years of development. All other cell and organ systems remain functional. The biological significance of human PNP is degradation of deoxyguanosine, and apoptosis of T-cells occurs as a consequence of the accumulation of deoxyguanosine in the circulation, and dGTP in the cells. Control of T-cell proliferation is desirable in T-cell cancers, autoimmune diseases, and tissue transplant rejection. The search for powerful inhibitors of PNP as anti-T-cell agents has culminated in the immucillins. These inhibitors have been developed from knowledge of the transition state structure for the reactions catalyzed by PNP, and inhibit with picomolar dissociation constants. Immucillin-H (Imm-H) causes deoxyguanosine-dependent apoptosis of rapidly dividing human T-cells, but not other cell types. Human T-cell leukemia cells, and stimulated normal T-cells are both highly sensitive to the combination of Imm-H to block PNP and deoxyguanosine. Deoxyguanosine is the cytotoxin, and Imm-H alone has low toxicity. Single doses of Imm-H to mice cause accumulation of deoxyguanosine in the blood, and its administration prolongs the life of immunodeficient mice in a human T-cell tissue xenograft model. Immucillins are capable of providing complete control of in vivo PNP levels and hold promise for treatment of proliferative T-cell disorders.

Keywords: Immucillin; Purine nucleoside phosphorylase; T-cell leukemia; Autoimmunity; Transition state; Apoptosis; Deoxyguanosine toxicity

1. Introduction

Purine nucleoside phosphorylase (PNP) catalyzes the reversible reactions [1]:

$$\text{(deoxy)guanosine} \qquad \text{guanine}$$
$$\text{(deoxy)inosine} + PO_4 \leftrightarrow \text{hypoxanthine} + \alpha - D$$
$$- \text{(deoxy)ribose 1} - PO_4$$

Prepared by her earlier discovery of severe combined immunodeficiency in adenosine deaminase deficiency, Eloise Giblett discovered that infants with a rare T-cell immunodeficiency lacked PNP [2]. Subsequent studies indicated that T-cell deficiency resulted from altered pathways of purine metabolism. Deoxyguanosine accumulates in the blood as a result of PNP deficiency, and is transported and phosphorylated by T-cell deoxynucleoside kinases to form pathologically elevated levels of dGTP specifically in these cells [3–6]. Inhibition of PNP was soon identified as a target for the regulation of undesirable T-cell proliferation, a campaign was launched for the discovery of powerful inhibitors [7]. Thirty-three patents for PNP inhibitors were listed by 1998, but clinical trials with the best of these inhibitors failed to show adequate inhibition to cause regulation of activated T-cells [8]. Type IV autoimmune disorders are a primary disease target for PNP inhibitors, and are caused by inappropriate activation of T-cells by self-antigens [9]. These disorders include rheumatoid arthritis, psoriasis, inflammatory bowel disorders and multiple sclerosis. In addition, T-cell leukemias and lymphomas would be primary proliferative targets for PNP inhibitors.

Inhibitor design for patented PNP inhibitors have used structure–activity relationships and structure-based design,

Abbreviations: PNP, purine nucleoside phosphorylase; Imm-H, Immucillin-H [(1*S*)-1-(9-deazahypoxanthin-9-yl)-1,4-dideoxy-1,4-imino-D-ribitol]; Imm-G, Immucillin-G [(1*S*)-1-(9-deazaguanin-9-yl)-1,4-dideoxy-1,4-imino-D-ribitol]; dNTP, 2′-deoxynucleoside 5′-triphosphates; K_i*, the equilibrium dissociation constant between an enzyme and inhibitor that includes a slow onset step; IL-2, interleukin-2; SCID mice, a mouse strain with genetically derived severe combined immunodeficiency; BCX-1777≡Immucillin-H

* Tel.: +1-718-430-2813; fax: +1-718-430-8565.
E-mail address: vern@aecom.yu.edu (V.L. Schramm).

0925-4439/02/$ - see front matter
PII: S0925-4439(02)00073-X

in which the catalytic site of PNP containing substrate or product analogues or weak inhibitors was sequentially filled with newly designed analogues followed by subsequent structural and kinetic characterization and refinement of catalytic site contacts [10,11]. The most powerful inhibitors obtained by these methods are in the low nanomolar range for inhibitory dissociation constants [8].

During this period, methods were also being developed for the experimental analysis of enzymatic transition states by kinetic isotope effect analysis [12–15]. Analogues that resemble enzymatic transition states capture the enzymatic forces used for catalysis and convert catalytic energy into binding energy, resulting in powerful inhibition [15–17]. The inversion of configuration at the anomeric carbon of PNP substrates suggested a nucleophilic displacement reaction, but compounds synthesized to resemble such transition states bound no better than substrates. The possibility of transition state inhibitor design for PNP became a reality in 1995, when the transition state structure was resolved from studies of the chemical mechanism and kinetic isotope effects [18–20]. This review provides a summary of the biology, enzymology and chemistry that led to the development of the immucillins, PNP inhibitors of sufficient specificity and affinity to cause deoxguanosine accumulation in mammals.

2. PNP in human nucleotide metabolism

The (deoxy)nucleoside substrates of PNP are normally absent from the blood as a result of robust PNP catalytic activity in the intestine, liver, erythrocytes, lymphocytes, spleen and kidney [21,22]. The activity of PNP in the blood alone causes injected nucleoside substrates to undergo phosphorolysis with a half-life of a few seconds. However, PNP substrates accumulate in the blood and urine of PNP-deficient patients, replacing uric acid, which is dramatically reduced in both blood and urine (summarized in Ref. [23]). This experiment of nature confirms that the pathway of purine nucleoside degradation requires PNP, and without it, nucleosides accumulate, purine bases for salvage pathways and degradation are depleted, and the rate of de novo purine synthesis increases [22]. Overproduction of purines is not accompanied by purine precipitation disorders in PNP deficiency since the (deoxy)nucleosides are more soluble than uric acid. Blood levels of these metabolites are significant and the primary purine excretion products are urinary nucleosides. In addition, (deoxy)nucleoside salvage increases because of excess substrate availability. Dividing T-cells express an active deoxycytidine kinase, whose normal role is the salvage of deoxycytidine to form dCMP → → dCTP for DNA synthesis in activated T-cells [24]. When deoxyguanosine accumulates beyond normal levels, deoxycytidine kinase accepts deoxguanosine to form dGMP → → dGTP. The allosteric inhibition site for dGTP on ribonucleotide diphosphate reductate inhibits cellular formation of dCDP and dUDP [25], thereby preventing DNA synthesis (Fig. 1).

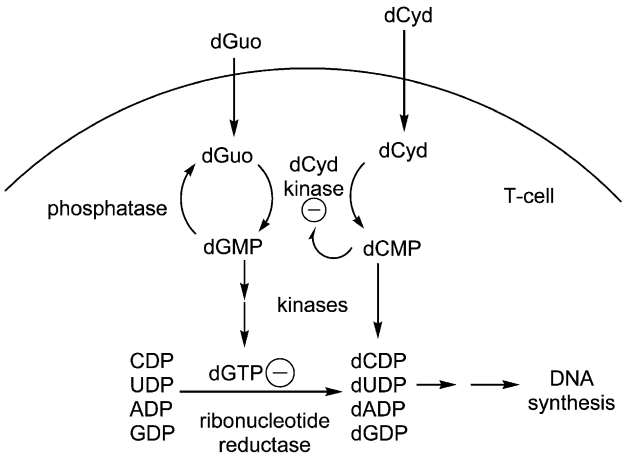

Fig. 1. Pathways of deoxyguanosine (dGuo) metabolism in human T-cells. The normal function of deoxycytidine (dCyd) kinase is salvage of dCyd arising from apoptosis of other T-cells. It is regulated by dCMP product inhibition. Excess dGuo is phosphorylated to dGMP by the same enzyme, but dGMP is not a good product inhibitor. Increased dGTP allosterically inhibits ribonucleotide reductase, preventing DNA synthesis and T-cell division.

Factors that have been proposed to make the disorder specific for T-cells include high capacity for deoxynucleoside transport, high expression levels of deoxycytidine kinase, and low levels of phosphatases for dGMP. The normal response to antigenic T-cell stimulation requires clonal expansion from a few cells with the appropriate receptors to the T-cell mass required for an activated T-cell response. This response requires rapid T-cell proliferation involving relatively large quantities of DNA synthesis. Activation of T-cells under conditions of unbalanced dNTPs induces apoptosis, and instead of T-cell proliferation, depletion of T-cells occurs [26]. T-cell populations are exquisitely poised for apoptotic responses, since ~ 99% of developing thymocytes do not receive an antigenic stimulatory response and undergo apoptosis under conditions of normal development [27].

Knowledge of human purine metabolism is required to understand PNP deficiency since the metabolism of deoxyguanosine differs between humans and mice. Mice made genetically deficient in PNP do not undergo T-cell depletion, and some of the cellular changes observed in the mice are attributed to the action of a mitochondrial deoxyguanosine kinase [28–30]. A useful outcome of this finding is that xenografts of human T-cells into mice allow analysis of the effects of PNP inhibitors with only modest effects on the host T-cell profile [31,32].

3. Catalytic properties of PNP

Mammalian PNPs catalyze the phosphorolysis of the natural 6-oxypurine (deoxy)nucleosides and are inactive against (deoxy)adenosine or the pyrimidine (deoxy)nucleosides [33]. The catalytic efficiency is high for the deoxy-

guanosine nucleoside that characterizes its biological function [1]. The homotrimer exhibits Michaelis–Menten initial rate kinetics and has no known physiologic regulatory sites. PNP is present at micromolar concentrations in blood cells and is coupled to a substrate trapping phenomenon known as catalytic commitment [14,19]. Every collision of a substrate (deoxy)nucleoside with the catalytic site leads to its trapping and conversion to product. With the high concentrations of enzyme, catalytic commitment, and low K_m value, cells containing high concentrations of PNP are assured of the virtual absence of free deoxyguanosine. Mitochondrial deoxyguanosine metabolism is exempt from this degree of deoxyguanosine removal since PNP is absent and a deoxyguanosine kinase is present [34]. Repair and recycling of mitochondrial DNA generates deoxguanosine that is proposed to remain in this compartment.

Under nonphysiological conditions, in the absence of phosphate, PNP catalyzes a slow hydrolysis of inosine in which the first catalytic site releases ribose, but binds tightly (1 pM) to the hypoxanthine product [18]. The enzyme stalls in a complex with hypoxanthine bound at one of the three catalytic sites, demonstrating sequential catalytic site action now made familiar from the action of F_1F_0 ATPase [35]. The relevance of sequential site catalytic action for cancer therapy is the prediction that inhibition of any single subunit of the PNP homotrimer will lead to full inactivation of catalytic activity. Immucillin-H (Imm-H) has been shown to act by this mechanism and one-third-the-sites inhibition is discussed in more detail in Section 5.

4. Transition state analysis and PNP

Chemical transition states occur within the lifetime of a single bond vibration, approximately 10^{-13} s, and direct observations have only been successful in gas-phase studies by laser spectroscopy [36]. Enzymatic transition states have similar lifetimes and can be established from intrinsic kinetic isotope effects by the experimental steps: (1) synthesis of substrates with specific atomic labels surrounding the bonds being made and broken in the transition state; (2) establish chemical or kinetic conditions where the catalytic step (transition state formation) is the first irreversible step in the catalytic cycle, or where intrinsic isotope effects can be obtained; (3) measure a family of kinetic isotope effects for the atoms whose bonding patterns are perturbed at the transition state; and (4) use bond vibrational analysis coupled to quantum chemistry predictions to match the kinetic isotope effects to the transition state structure. Geometric and electrostatic properties of the transition state can be used as an atomic blueprint to design stable analogues. Chemical synthesis of the transition state analogues provides the desired inhibitors for enzymatic and biological testing against the target. The experimental implementation of these steps has been outlined in reviews [14,37–39], and will be exemplified here with the example of PNP.

PNP demonstrated no kinetic isotope effects with inosine and phosphate as substrates, because of catalytic commitment, and bound products reforming substrates on the enzyme prior to product release [19]. Intrinsic isotope effects were established using the hydrolytic reaction, where catalysis is slow and no back-reaction occurs, and also with arsenate (AsO_4) as a phosphate analogue [20]. Arsenate reacts to form α-D-ribose 1-arsenate, an unstable intermediate that hydrolyzes rapidly and prevents the products of the reaction from reforming as substrates prior to release from the enzyme. The intrinsic isotope effects were used to establish the transition state features

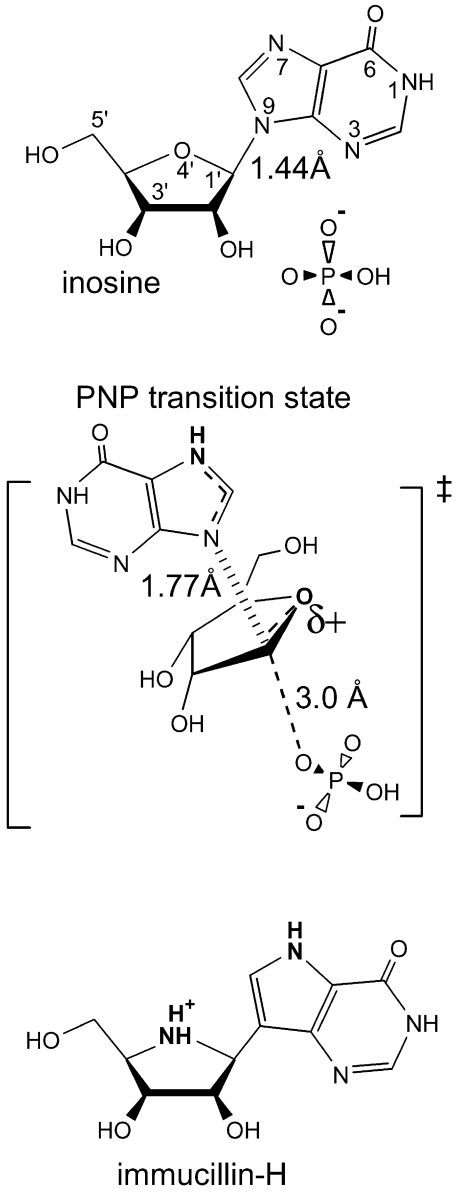

Fig. 2. Substrate (inosine), transition state and transition state inhibitor (Imm-H) for PNP. The geometry of the transition state is shown looking at C1′ of the ribosyl ring. Features of the transition state are highlighted in bold, and also appear in the inhibitor [51].

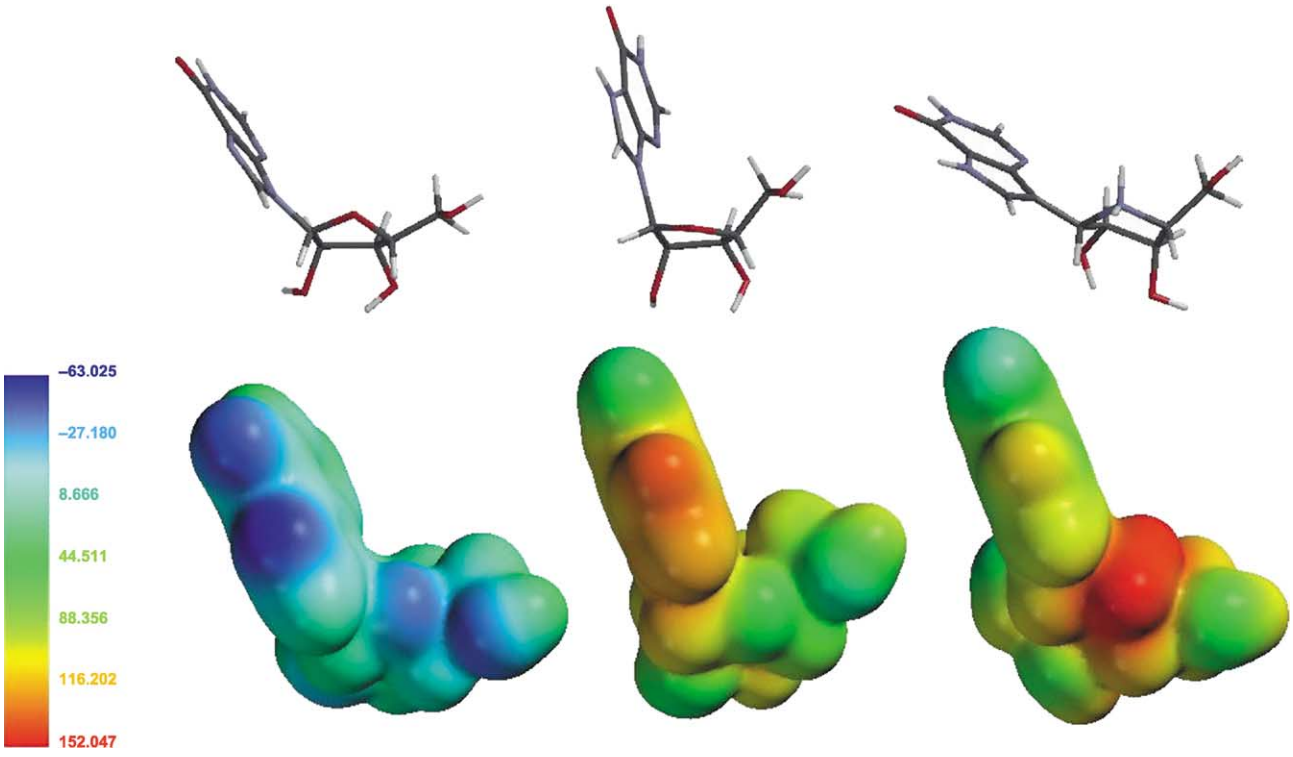

Fig. 3. Molecular electrostatic potential surfaces for inosine, the transition state of PNP and Imm-H. The geometry around the 5′-hydroxymethyl group and the ribosidic-base torsion angles were fixed at the values established from the X-ray crystallographic studies. In the transition state, N7 was protonated and the N9–C1′ bond was fixed at 1.8 Å. The electron distribution was calculated using Gaussian 98 with the STO-3G basis set.

of 0.38 Pauling bond order to the hypoxanthine leaving group, protonation or hydrogen-bond stabilization to N7 of the purine, van der Waals contact to the attacking phosphate nucleophile, and conversion of the ribosyl group to a partially charged ribooxacarbenium ion [20]. The results established that the chemical property of the transition state is dissociative, rather than the associative property expected for a symmetric nucleophilic displacement (Fig. 2). The results provided the first sufficiently complete structure of the transition state to permit the design of transition state inhibitors. These features were also consistent with the transition states established for other purine N-ribohydrolases [40,41], and with an earlier isotope effect measured for the PNP from *Escherichia coli* [42].

5. Imm-H design and synthesis

The features of the transition state structure for PNP were used to design a chemically stable isologue (same molecular shape and volume) to act as transition state analogue inhibitor (Fig. 2). Inosine was the substrate for transition state analysis, and the transition state inhibitor was designed to mimic this transition state. The ribosyl group at the transition state is a partially positively charged ribooxacarbenium ion, and was mimicked in Imm-H with an iminoribitol structure. In Imm-H, the imino group[1] is protonated with a pK_a of 6.5, providing a partial positive charge at physiological pH values. The bond to the leaving group purine is more than 60% dissociated at the transition state, causing the pK_a at N7 of the purine to increase. Immucillins were designed with a carbon–carbon ribosidic link to provide chemical stability relative to the carbon–nitrogen link in normal substrates. This carbon–ribosidic bond also changes the bond conjugation pattern of the inhibitor, increasing the pK_a of N7 from ~ 2 in inosine to ~ 9 in Imm-H. The pK_a of this group at the transition state has not been measured, but is elevated toward 7 or above as the ribosidic bond is broken. Nitrogen-7 is proposed to be a site of protonation or hydrogen bonding by the enzyme to form the transition state, since the bonding electrons must be accommodated in the leaving group and protonation at N7 or a favorable H-bond at this site assists in electron departure from the N-ribosidic bond. The elevated pK_a at this site constitutes one of the transition state features. The ability of N7-methyl substituted inosine and guanosine molecules to act as substrates of PNP [43] indicates that the Asn243 that H-bonds to this site is sufficiently flexible to accommodate an N7-methyl substituent. The methyl group provides a similar

[1] The IUPAC nomenclature for the ring nitrogen in sugar analogues accepts amino or imino. The original description of the deoxyiminoribitols [64] used the imino nomenclature, which we maintain here.

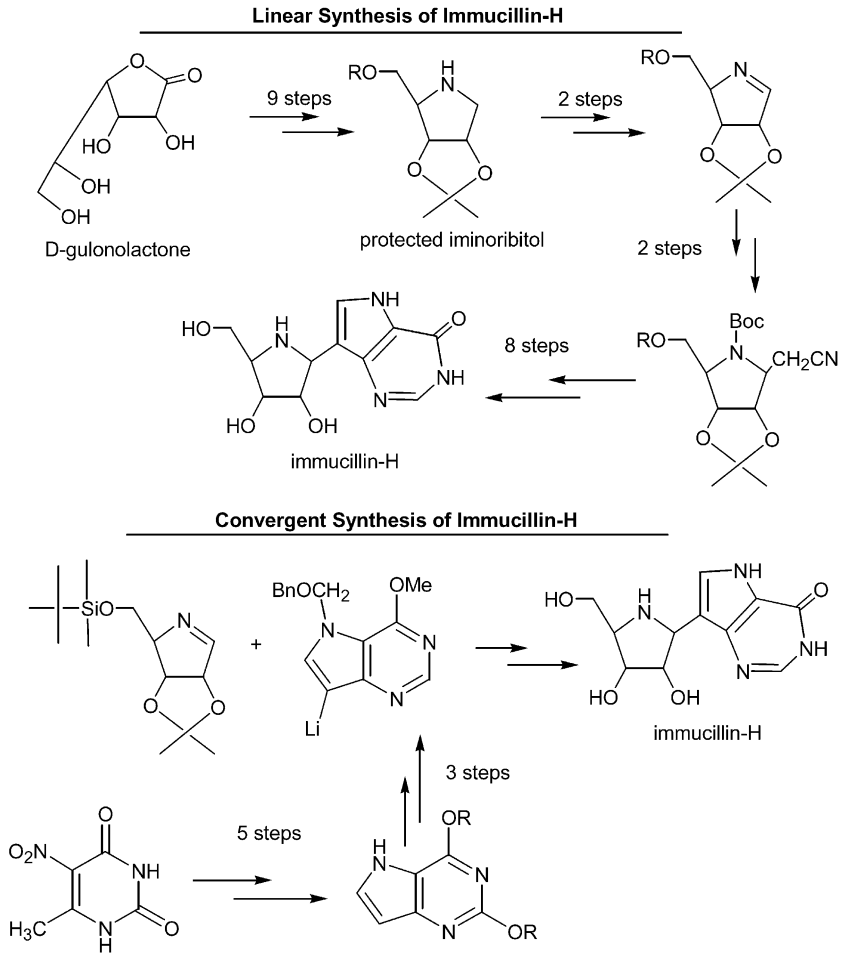

Fig. 4. Chemical synthesis of Imm-H by the linear and convergent pathways. These methods have been published and details of synthesis are provided in Refs. [48,50].

electronic effect in assisting the purine to accept bonding electrons.

The atomic replacements between inosine and Imm-H make an insignificant change in atomic size, but a dramatic change in the molecular electrostatic potential surface[2] (Fig. 3) [44]. Analysis of the molecular electrostatic potential surface similarity between transition state and transition state inhibitors for several enzymes have established that this and the atomic size correlate with the affinity between enzyme and inhibitor [45,46]. A departure from other inhibitor design programs was to eliminate features of the phosphate anion. Transition state analysis revealed that phosphate is not bonded at the transition state, but is in van der Waals contact, with less than 2% covalent bond order [20]. This finding established that the nucleoside contacts dominate transition state interactions, and that the phosphate binding site will fill with inorganic phosphate, an abundant component of cells.

[2] The molecular electrostatic potential surface is the force observed by a point charge at every location on the van der Waals surface of the molecule [44].

Chemical synthesis of Imm-H was first accomplished in a linear sequence of over 20 steps, beginning with D-gulonolactone, and based on the precedents of aryl and alkyl 1-substituted iminoribitols [47,48] and for synthesis of 9-deazapurine nucleosides [49] (Fig. 4). This synthetic procedure builds the protected iminoribitol from D-gulonolactone, followed by the stepwise addition of the components of the 9-deazahypoxanthine and deprotection. The chemical stability of the compound is revealed in the final deprotection step, reflux in concentrated HCl. Although this route provided the first access to Imm-H and Imm-G (the 9-deazaguanine analogue), it was not suitable for large-scale synthesis. An improved synthetic route produced activated and protected iminoribitol and 9-deazahypoxanthine in separate procedures, followed by reaction of the two halves of the molecule [50] (Fig. 4).

6. Inhibition of PNPs by Imm-H

Imm-H and Imm-G inhibited both bovine and human PNP, and exhibited the characteristics of slow-onset tight-

binding inhibitors [51]. Slow-onset inhibitors bind as reversible competitive ligands, followed by an isomerization of the enzyme that causes increased inhibitor binding affinity [52]. The initial binding phase for the bovine enzyme exhibits a K_i of 41 nM, followed by a time-dependent, slow onset ($k_5 = 0.06\ s^{-1}$) increase of affinity by a factor of 2000, to give a K_i* of 23 pM (Fig. 5). For the human enzyme, the initial binding phase is rapid, and the K_i* value is 72 pM (Table 1). The affinity of Imm-H is approximately one million times that for the inosine substrate. The size and molecular electrostatic potential properties of the inhibitor are similar to the transition state [51]. Binding affinity is dictated by on and off rates, in the case of tight-binding inhibitors, that for k_5 and k_6, the conformational changes that provide entry and departure from the tightly bound transition state analogue complex (Fig. 5). Release of Imm-

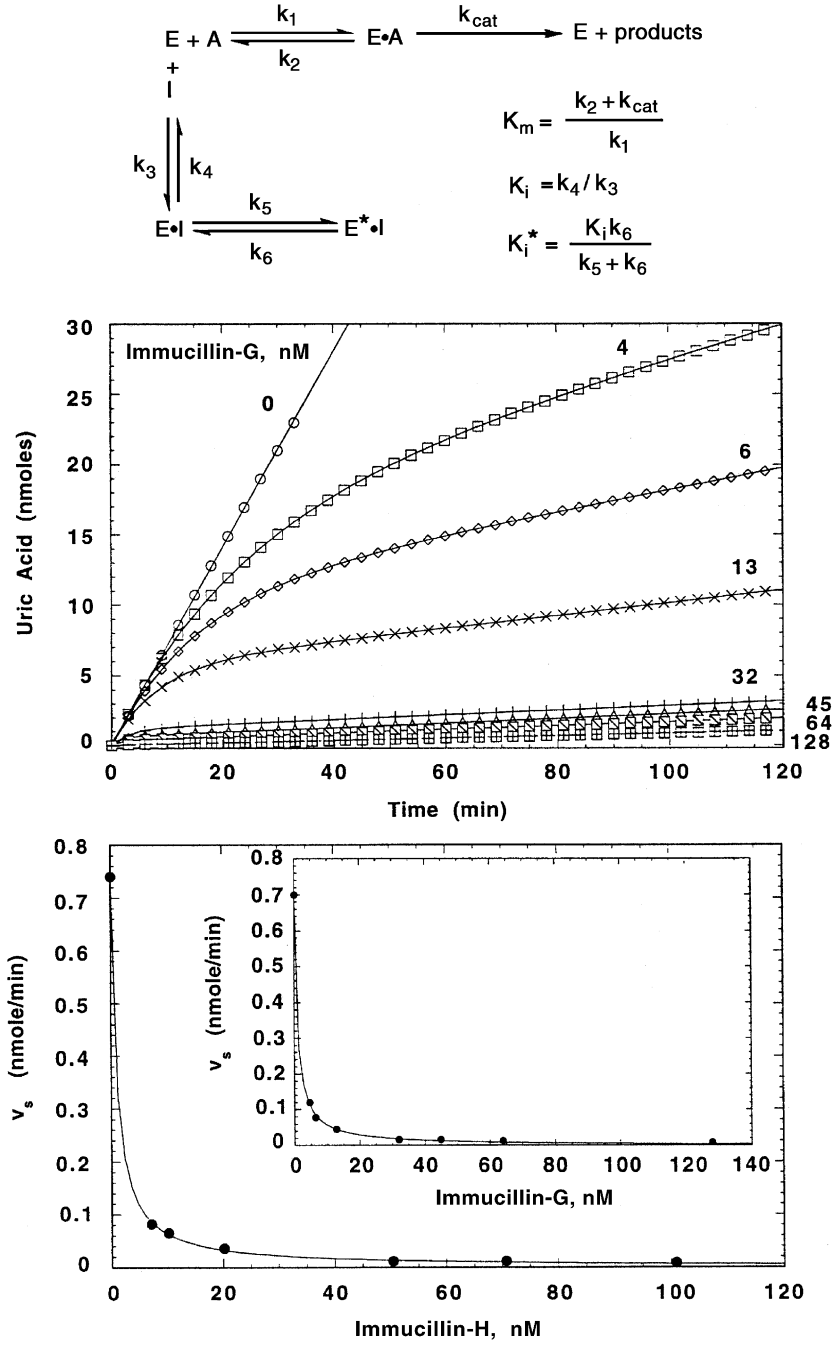

Fig. 5. The kinetics of PNP inhibition by Imm-G and Imm-H. E, A, P and I represent PNP, inosine, products and Imm-H or Imm-G, respectively. The rate constants k_5 and k_6 are the rate constants for formation of E*·I and its conversion to E·I. E·I is the rapidly reversible, weakly bound inhibitor and E*·I represents a conformational change that accompanies tight-binding of the inhibitor. The center panel demonstrates the slow-onset of inhibition, and the bottom panel demonstrates the post-slow onset rate (v_s) as a function of inhibitor concentration using inosine at a concentration of 200 times its K_m value. The reactions were coupled to xanthine oxidase to yield uric acid as product. Adapted from reference [51].

Table 1
Inhibition of PNPs by Imm-H

PNP source	K_i* (pM)	K_m (μM)	K_m/K_i
Human	73	40[a]	550,000
Bovine	23	17[a]	740,000
Mycobacterium tuberculosis	28	26[b]	930,000
Plasmodium falciparum	600	5[a]	8000

[a] The K_m values for inosine.
[b] The K_m values for 6-thio-7-methylguanosine.

H from the bovine enzyme has a $t_{1/2}$ of 5 h, compared to that from the human enzyme of 8 min. Inhibition was correlated with moles of Imm-H bound per trimeric enzyme, and the results established that binding of one Imm-H molecule per trimer, with the affinity described above, is responsible for the inhibition [51]. These inhibitory and binding studies established that Imm-H was the most powerful PNP inhibitor yet described. It acts by complete inhibition of PNP catalytic activity by filling only one of the three catalytic sites of the trimer of PNP [51]. This result was unexpected based on earlier kinetic studies and the previous X-ray crystal structures of PNP, all of which indicated equivalent, noninteracting sites in a symmetric trimer with identical subunit occupancy with substrate and inhibitor analogues [53]. Binding studies of Imm-H to bovine PNP indicated that filling of the first subunit is responsible for the inhibition, and occurs with the highest affinity, followed by saturation of the second and third sites with affinity orders of magnitude lower than the first subunit [54]. However, at large Imm-H excess, all three sites can be occupied. The impact of the partial-sites inhibition for cancer therapy is that physiological inhibition of PNP activity can be achieved with only one molecule of inhibitor bound for every three PNP subunits.

Although other applications of PNP inhibitors are beyond the scope of this review, Imm-H is also a powerful inhibitor of PNP from *M. tuberculosis* and *P. falciparum* [55,56] (Table 1). The crystal structure of *M. tuberculosis* has been solved with Imm-H and phosphate binding, revealing that this enzyme is similar to the mammalism enzyme [57]. In contrast, the PNP from *P. falciparum* is more closely related to the hexameric *E. coli* PNP, and has a lower affinity for Imm-H. Despite the lowered affinity, the addition of Imm-H to cultures of human erythrocytes infected with *P. falciparum* causes purine-less death of the parasites under physiological culture conditions [58].

7. Structure of PNP·Imm-H·PO_4

Crystals of bovine PNP with Imm-H and phosphate at the catalytic sites were grown in the presence of large excesses of phosphate and of Imm-H to saturate the catalytic sites [59]. The crystals, demonstrated uniform catalytic site filling at all three sites, and permitted the collection of the highest resolution data (1.5 Å) obtained for a complex of the bovine enzyme. The structure was compared to structures of bovine PNP solved earlier [53], to reveal the structural changes as the enzyme progresses from the Michaelis complex to the transition state and product complexes. Imm-H is situated in the catalytic sites similar to the position of inosine, except that contacts to the enzyme are closer to most parts of the complex (Fig. 6). Comparison of substrate, Imm-H and product complexes to the actual transition state structure docked into the catalytic site permitted analysis of the atomic motion that occurs as substrates are converted to products, and the analysis of the similarity between Imm-H and the docked transition state.

One surprising result is that the reaction occurs by unprecedented atomic motion in the reaction coordinate. These steps include; (a) enzymatic immobilization of the purine ring and phosphate, (b) generation of the ribooxacarbenium ion transition state with the participation of neighboring group oxygens from phosphate and the 5′-hydroxyl to stabilize the ribooxacarbenium ion and (c) migration of the C1′ anomeric carbon over the relatively long distance of 1.7 Å between the enzymatically stabilized nucleophiles, while the 5′-region of the ribosyl group remains immobile. This mechanism is a departure from solution chemistry, and also occurs in other ribosyltransferases. This mechanism has been called a nucleophilic displacement by electrophilic migration, and reflects the ability of enzymes to accomplish atomic motion of reactive groups in the protected environment of the catalytic site, (exemplified here by the ribooxacarbenium ion) [59,60]. A second important lesson of the study was that the transition state analogue and the actual transition state occupy the same positions, except for the 0.4 Å difference in structures resulting from the C–C covalent bond in the transition state analogue [59]. A third surprise from the structure with Imm-H involves the nature of the enzymatic activation of the leaving group purine and the formation of the ribooxacarbenium ion. Enzyme-immobilized water oxygens form a proton transfer bridge to solvent and provide the protons required for a H-bond and a protonation of the leaving group hypoxanthine. Activation of the leaving group occurs by; (a) a hydrogen bond to N7 shared to the side-chain carbonyl oxygen of Asn243, where the H-bonded proton is provided by the water bridge, and (b) protonation of O6 by an immobilized water that is sandwiched between O6 and Glu201. Near-optimal contacts at every H-bond donor/acceptor pair on Imm-H and phosphate at the catalytic site indicated that improvement on the binding affinity by changing the structure of the immucillins might be difficult.

8. Effect of Imm-H on transformed and activated T-cells

Human T-cell immunodeficiency from PNP loss is completely dependent on the presence of deoxyguanosine and its

conversion to dGTP [31,32]. Cultures of human T-cell leukemia lines were tested for growth in the presence of Imm-H with and without deoxyguanosine (Fig. 7). The selective inhibition of T-cells, only in the presence of deoxyguanosine, established that Imm-H is biologically available, and is dependent on deoxyguanosine. Analysis of treated cells established that Imm-H with deoxyguanosine caused the accumulation of dGTP [31]. Under conditions of 20 μM deoxyguanosine in the medium, the IC_{50} for Imm-H was 0.4 to 5 nM for reduction of thymidine incorporation in cells cultured for 3 days (Fig. 7). The toxicity of Imm-H and deoxyguanosine is rescued by deoxycytidine, a metabolite known to prevent dGTP accumulation by substrate competition for deoxycytidine kinase and by dCMP product inhibition of the enzyme [61] (Fig. 7C). Seventeen non-T-cell lines were unaffected by Imm-H at 10 μM, several thousand-fold above the effective dose for human leukemic T-cells [31]. T-cells isolated from normal human volunteers are not affected by Imm-H unless they are stimulated to divide, and show increasing sensitivity with increased stimulation [31,32] (Fig. 8). Peripheral human T-cells stimulated to rapid division by excess interleukin-2 (IL-2) and mononuclear cells were inhibited by Imm-H and deoxguanosine with an IC_{50} value of 5 nM. The results demonstrate that inhibition of PNP by

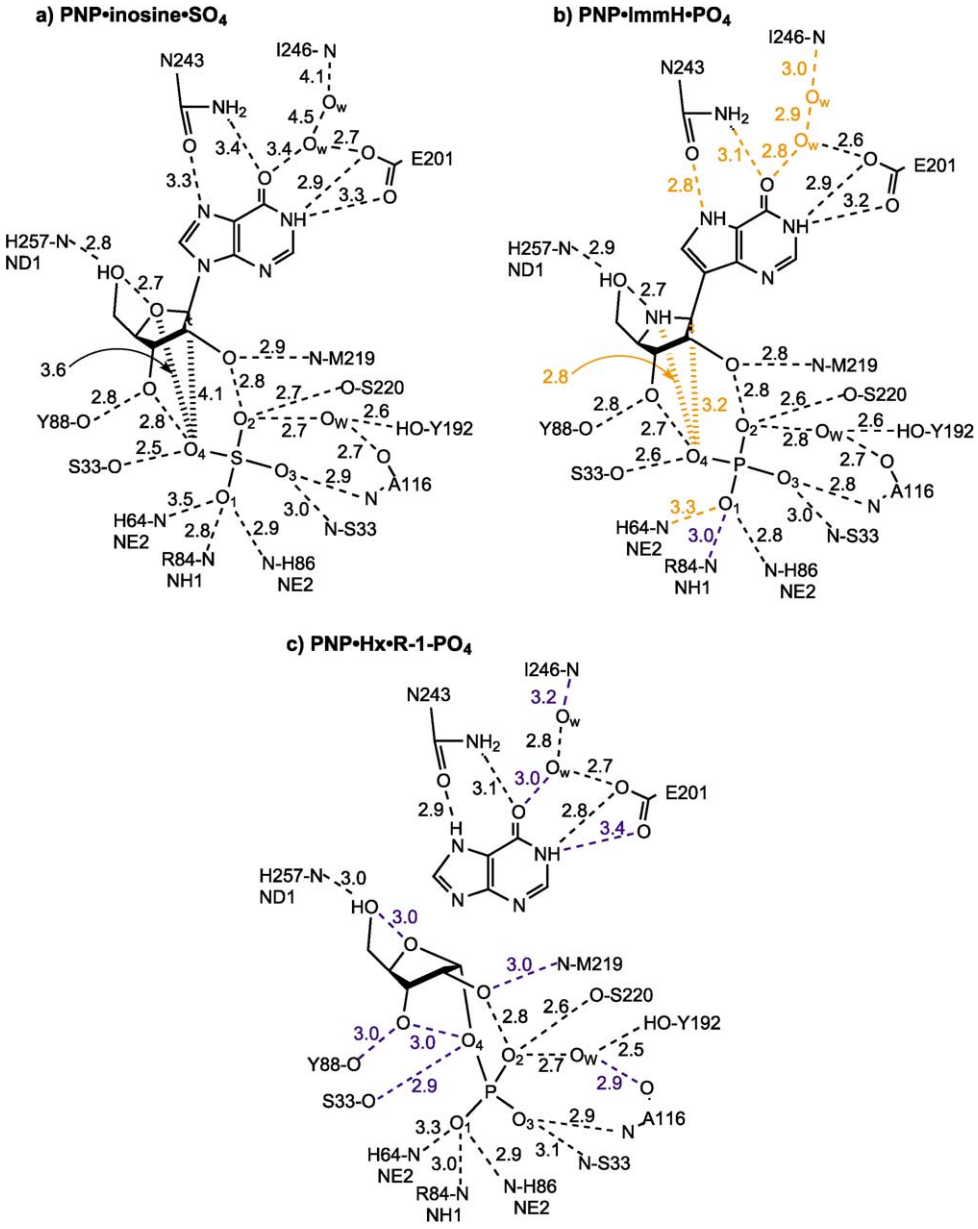

Fig. 6. The structures of bovine PNP with substrate analogues (inosine + SO_4), transition-state complex (Imm-H + PO_4) and products (hypoxanthine + ribose 1-PO_4) bound at the catalytic sites. Substrate and product complexes are from Ref. [53], and this figure is reproduced from Ref. [59]. Hydrogen bond distances are shown in angstroms. Red indicates bonds that shorten significantly and blue indicates bonds that lengthen significantly in the conversion of (a) to (b), and of (b) to (c).

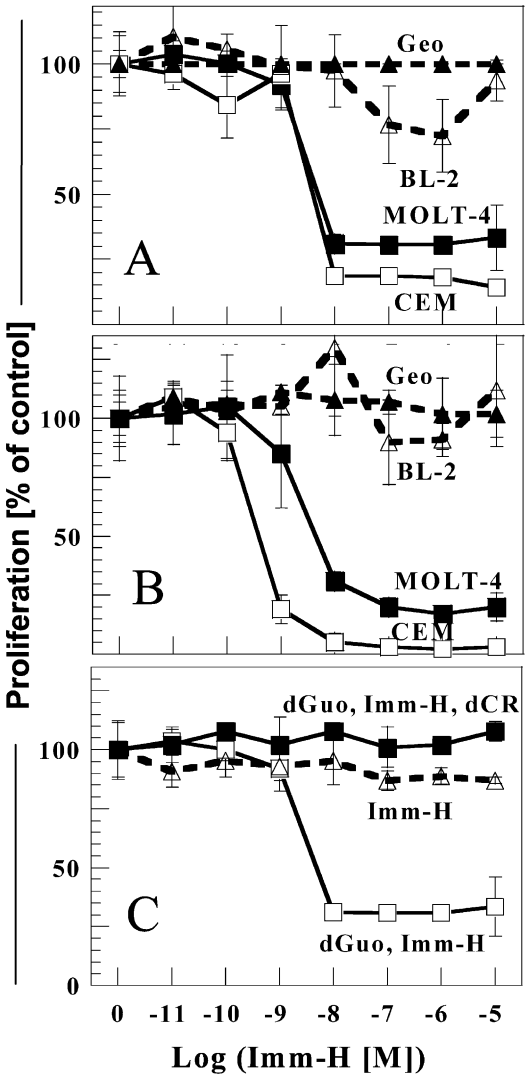

Fig. 7. The inhibition of human T-cell leukemia lines by Imm-H and deoxyguanosine. MOLT-4 and CEM are human T-cell leukemia cell lines, while Geo is a human colon carcinoma cell line and BL-2 is a human B-cell leukemia cell line. Panel A demonstrates the response of cell lines to 20 μM deoxyguanosine and the indicated concentrations of Imm-H after 3 days of culture and analysis of cell activity by the viability dye WST-1. Panel B is the same experiment, but with cell viability tested by tritium–thymidine incorporation. Panel C demonstrates that Imm-H alone has no effects on CEM cell viability, and that deoxycytidine (dCR) rescues against the effects of Imm-H and deoxyguanosine by the mechanism shown in Fig. 1. This figure is reproduced from Ref. [31].

Imm-H is sufficient to cause dGTP accumulation and to induce apoptosis specifically in rapidly dividing T-cells.

9. Imm-H in mice and effects on T-cell xenografts

Bioavailability of Imm-H was tested in mice by a comparison of oral and injected doses, and established that oral availability is high, at 63% of the injected dose [32]. A key test of the biological effectiveness of the inhibitor is the ability to increase the concentration of deoxyguanosine in

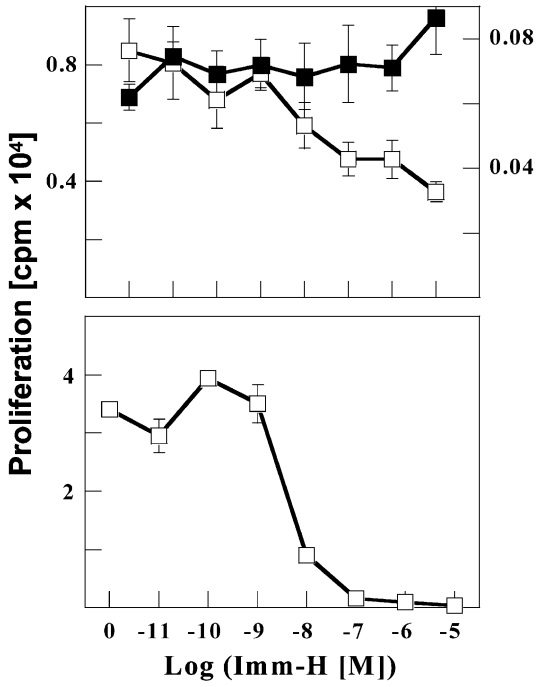

Fig. 8. The effect of Imm-H on [^{3}H]thymidine incorporation by human T-lymphocytes. Reproduced from Ref. [31]. In the top panel, peripheral T-cells from four donors were incubated for 3 days with no stimulation (solid squares) or with physiological levels of IL-2. In the bottom panel, cells were treated with excess IL-2 and mitomycin-treated mononuclear cells, followed by 6-day incubation. Error bars represent the results averaged for the T-cells of four donors.

blood. Both humans and mice have high concentrations of PNP in erythrocytes; therefore, deoxyguanosine is not present at detectable levels in the blood. A single oral dose of 10 mg/kg Imm-H to mice increased the plasma concen-

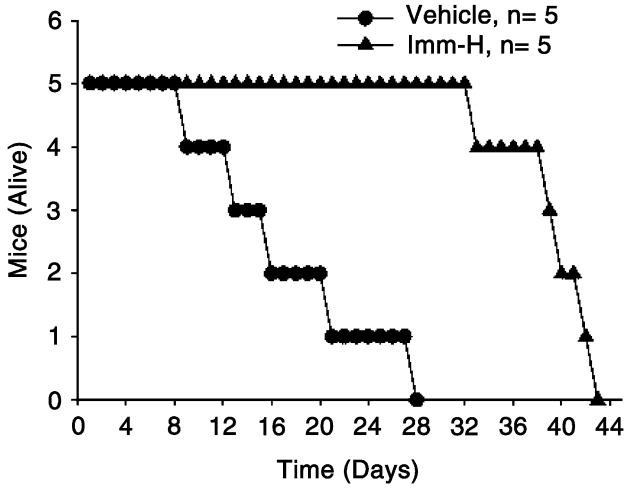

Fig. 9. The effect of Imm-H on the human lymphocyte–mouse xenograft tissue rejection model. The results are reproduced from Ref. [32]. SCID (hu-PBL) mice were treated with 20 mg/kg Imm-H for 5 days, and the natural killer lymphocytes depleted with anti-ASGMI antibodies. Mice were irradiated and human buffy coat cells were injected. The group with Imm-H treatment (triangles) survived approximately twice as long as the control group.

tration of deoxyguanosine to a peak concentration of 5 μM over a period of 3 h, establishing in vivo efficacy for whole-body PNP inhibition in the mouse [32]. Elevated deoxyguanosine also occurs in the human genetic deficiency of PNP, and plasma levels are reported to be in the range of 3 to 17 μM [23]. Thus, a single oral dose of Imm-H to mice can achieve a deoxyguanosine concentration that is adequate to cause T-cell deficiency in humans. These experiments were a prelude to the use of a mouse model of human immune transplantation rejection that has been developed and extended to SCID mice [62,63]. In this protocol, human peripheral blood lymphocytes (PBLs) are engrafted into SCID mice, and are stimulated to divide by the host antigens. Expansion of the human PBL cells causes the SCID mice to die from xenogenic graft vs. host disease, approximately 4 weeks after engraftment. Death is caused by infiltration of human lymphocytes into the tissues of the host mouse. The effects of Imm-H were tested by pretreating mice with Imm-H to elevate the deoxyguanosine levels, followed by engraftment and continued treatment with Imm-H to determine effects on life span. Control animals were treated in the same way, except that no Imm-H was given. The results demonstrated a two-fold increase in life span compared to control mice (Fig. 9) [32]. These results establish the ability of Imm-H to influence human T-cell proliferation in the mouse model of host vs. graft disease, and therefore the ability to obtain sufficient inhibition of whole body PNP to sustain elevated deoxguanosine levels.

10. Prospectus for applications of Imm-H

Based on the enzymology, cell culture and animal model work published to date, the prospects for Imm-H to function as an in vivo anti-T-cell agent are the most encouraging yet obtained in the 26 years since Eloise Giblett discovered the genetic deficiency of PNP [2]. Recent studies on the mouse model of Imm-H immunosuppression of human T-cells concluded with the statement that this inhibitor is the first known example of a PNP inhibitor that elevates deoxyguanosine in mice similar to the levels observed in PNP-deficient patients [32]. Phase I/II clinical trials of Imm-H against human T-cell leukemia have been initiated under the trade name of BCX-1777.

Acknowledgements

Research in this laboratory is supported by research grants from the National Institutes of Health. Greg Kicska and Robert Miles have been instrumental in the research on PNP and Imm-H in this laboratory. Alexander Fedorov, Wuxian Shi and Steven Almo are responsible for the X-ray crystallography. Richard Furneaux and Peter Tyler of Industrial Research, New Zealand, pioneered the synthesis of Imm-H, and Shanta Bantia of BioCryst has had a central role in cellular and animal studies. The author thanks Brett Lewis for help in preparing figures.

References

[1] J.D. Stoeckler, C. Cambor, R.E. Parks Jr., Biochemistry 19 (1980) 102–107.
[2] E.R. Giblett, A.J. Ammann, D.W. Wara, R. Sandman, L.K. Diamond, Lancet 1 (1975) 1010–1013.
[3] T.A. Krenitsky, J.V. Tuttle, G.W. Koszalka, I.S. Chen, L.M. Beachman, J.L. Rideout, G.B. Elion, J. Biol. Chem. 251 (1976) 4055–4061.
[4] D.A. Carson, J. Kaye, J.E. Seegmiller, Proc. Natl. Acad. Sci. U. S. A. 74 (1977) 5677–5681.
[5] B.S. Mitchell, E. Mejias, P.E. Daddona, W.N. Kelly, Proc. Natl. Acad. Sci. U. S. A. 75 (1978) 5011–5014.
[6] B. Ullman, L.J. Gudas, S.M. Clift, D.W. Martin Jr., Proc. Natl. Acad. Sci. U. S. A. (1979) 1074–1078.
[7] S.E. Ealick, Y.D. Babu, C.E. Bugg, M.D. Erion, W.C. Guida, J.A. Montgomery , J.A. Secrist III, Proc. Natl. Acad. Sci. U. S. A. 88 (1991) 11540–11544.
[8] P.E. Morris, J.A. Montgomery, Expert Opin. Ther. Pat. 8 (1998) 283–299.
[9] C.A. Janeway Jr., P. Travers, Immunobiology: The Immune System in Health and Disease, 3rd edn., Current Biology/Garland Publishing, London and New York, 1997.
[10] M.D. Erion, S. Niwas, J.D. Rose, S. Ananthan, M. Allen, J.A. Secrist III, Y.S. Babu, et al., J. Med. Chem. 36 (1993) 3771–3783.
[11] W.C. Guida, R.D. Elliott, H.J. Thomas, J.A. Secrist III, Y.S. Babu, C.E. Bugg, M.D. Erion, S.E. Ealick, J.A. Montgomery, J. Med. Chem. 37 (1994) 1109–1114.
[12] J. Rodgers, D.A. Femec, R.J. Schowen, J. Am. Chem. Soc. 104 (1982) 3263–3268.
[13] W.W. Cleland, Methods Enzymol. 87 (1982) 625–641.
[14] D.B. Northrop, Biochemistry 14 (1975) 2644–2651.
[15] V.L. Schramm, Ann. Rev. Biochem. 67 (1998) 693–720.
[16] W.P. Jencks, Adv. Enzymol. 43 (1975) 219–410.
[17] R. Wolfenden, Nature 223 (1969) 704–705.
[18] P.C. Kline, V.L. Schramm, Biochemistry 31 (1992) 5964–5973.
[19] P.C. Kline, V.L. Schramm, Biochemistry 32 (1993) 13212–13219.
[20] P.C. Kline, V.L. Schramm, Biochemistry 34 (1995) 1153–1162.
[21] H.A. Simmonds, L.D. Fairbanks, G.S. Morris, G. Morgan, A.R. Watson, P. Timms, B. Singh, Arch. Dis. Child. 62 (1987) 385–391.
[22] A. Cohen, D. Doyle, D.W. Martin Jr., A.J. Ammann, N. Engl. J. Med. 295 (1976) 1449–1454.
[23] M.S. Hershfield, B.S. Mitchell, in: C.R. Scriber, A.L. Beaudet, W.S. Sly, D. Valle (Eds.), The Metabolic Basis of Inherited Disease, 8th edn., McGraw-Hill, NY, 2001, pp. 2585–2624, Chapter 109.
[24] N.S. Datta, D.S. Shewach, B.S. Mitchell, I.H. Fox, J. Biol. Chem. 264 (1989) 9359–9364.
[25] L. Thelander, P. Reichard, Ann. Rev. Biochem. 48 (1979) 133–158.
[26] M.L. Agarwal, A. Agarwal, W.R. Taylor, O. Chernova, Y. Sharma, G.R. Stark, Proc. Natl. Acad. Sci. U. S. A. 95 (1998) 14775–14780.
[27] C.D. Surh, J. Sprent, Nature 372 (1994) 100–103.
[28] E.R. Mably, E. Fung, F.F. Snyder, Genome 32 (1989) 1026–1032.
[29] F.F. Synder, J.P. Jenuth, E.R. Mably, R.K. Mangat, Proc. Natl. Acad. Sci. U. S. A. 94 (1997) 2522–2527.
[30] E. Arpaia, P. Benveniste, A. Di Cristofano, Y. Gu, I. Dalal, S. Kelly, M. Hershfield, et al., J. Exp. Med. 191 (2000) 2197–2208.
[31] G.A. Kicska, K. Long, H. Hörig, C. Fairchild, P.C. Tyler, R.H. Furneaux, V.L. Schramm, H.L. Kaufman, Proc. Natl. Acad. Sci. U. S. A. 98 (2001) 4593–4598.
[32] S. Bantia, P.J. Miller, C.D. Parker, S.L. Ananth, L.L. Horn, J.M. Kilpatrick, P.E. Morris, T.L. Hutchison, J.A. Montgomery, J.S. Sanduh, Int. Immunopharmacol. 1 (2001) 1199–1210.

[33] B.K. Kim, S. Cha, R.E. Parks Jr., J. Biol. Chem. 243 (1968) 1763–1770.
[34] E. Arpaia, P. Benveniste, A. Di Cristofano, Y. Gu, I. Dalal, S. Kelly, M. Hershfield, P.P. Pandolfi, C.M. Roifman, A. Cohen, J. Exp. Med. 191 (2000) 2197–2207.
[35] P.D. Boyer, Ann. Rev. Biochem. 66 (1997) 717–749.
[36] D. Zhong, S. Ahmad, P.Y. Cheng, A.H. Zewail, J. Am. Chem. Soc. 119 (1997) 2305–2306.
[37] V.L. Schramm, Methods Enzymol. 308 (1999) 301–355.
[38] P.J. Berti, Methods Enzymol. 308 (1999) 355–397.
[39] B.B. Braunheim, S.D. Schwartz, Methods Enzymol. 308 (1999) 398–426.
[40] B.A. Horenstein, D.W. Parkin, B. Estupinan, V.L. Schramm, Biochemistry 30 (1991) 10788–10795.
[41] F. Mentch, D.W. Parkin, V.L. Schramm, Biochemistry 26 (1987) 921–930.
[42] R.L. Stein, E.H. Cordes, J. Biol. Chem. 256 (1981) 767–772.
[43] A. Bzowaka, E. Kulikowska, E. Darzynkiewicz, D. Shugar, J. Biol. Chem. 263 (1988) 9212–9217.
[44] B.A. Horenstein, V.L. Schramm, Biochemistry 32 (1993) 9917–9925.
[45] C.K. Bagdassarian, V.L. Schramm, S.D. Schwartz, J. Am. Chem. Soc. 118 (1996) 8825–8836.
[46] B.B. Braunheim, R.W. Miles, V.L. Schramm, S.D. Schwartz, Biochemistry 38 (1999) 16076–16083.
[47] B.A. Horenstein, R.F. Zabinski, V.L. Schramm, Tetrahedron Lett. 34 (1993) 7213–7216.
[48] G.B. Evans, R.H. Furneaux, G.J. Gainsford, V.L. Schramm, P.C. Tyler, Tetrahedron 56 (2000) 3053–3062.
[49] M.I. Lin, W.Y. Ren, B.A. Otter, R.S. Kline, J. Org. Chem. 48 (1983) 780–788.
[50] G.B. Evans, R.H. Furneaux, T.L. Hutchison, H.S. Kezar, P.E. Morris, V.L. Schramm, P.C. Tyler, J. Org. Chem. 66 (2001) 5723–5730.
[51] R.W. Miles, P.C. Tyler, R.H. Furneaux, C.K. Bagdassarian, V.L. Schramm, Biochemistry 37 (1998) 8615–8621.
[52] J.F. Morrison, C.T. Walsh, Adv. Enzymol. Relat. Areas Mol. Biol. 61 (1988) 201–301.
[53] C. Mao, W.J. Cook, M. Zhou, A.A. Fedorov, S.C. Almo, S.E. Ealick, Biochemistry 37 (1998) 7135–7146.
[54] F. Wang, R.W. Miles, G.A. Kicska, E. Nieves, V.L. Schramm, R.H. Angeletti, Protein Sci. 9 (2000) 1660–1668.
[55] L.A. Basso, D.S. Santos, W. Shi, R.H. Furneaux, P.C. Tyler, V.L. Schramm, J.S. Blanchard, Biochemistry 40 (2001) 8196–8203.
[56] G.A. Kicska, P.C. Tyler, G.B. Evans, R.H. Furneaux, K. Kim, V.L. Schramm, J. Biol. Chem. 277 (2002) 3219–3225.
[57] W. Shi, L.A. Basso, D.S. Santos, P.C. Tyler, R.H. Furneaux, J.S. Blanchard, S.C. Almo, V.L. Schramm, Biochemistry 40 (2001) 8204–8215.
[58] G.A. Kicska, P.C. Tyler, G.B. Evans, R.H. Furneaux, V.L. Schramm, K. Kim, J. Biol. Chem. 277 (2002) 3226–3231.
[59] A. Fedorov, W. Shi, G.A. Kicska, E. Fedorov, P.C. Tyler, R.H. Furneaux, J.C. Hanson, G.J. Gainsford, J.Z. Larese, V.L. Schramm, S.C. Almo, Biochemistry 40 (2001) 853–860.
[60] V.L. Schramm, W. Shi, Curr. Opin. Struct. Biol. 11 (2001) 657–665.
[61] W.R. Osborne, C.R. Scott, Biochem. J. 214 (1983) 711–718.
[62] D.E. Mosier, R.J. Guilizia, S.M. Baird, D.B. Wilson, Nature 335 (1988) 256–259.
[63] J.S. Sandhu, R. Gorczynski, B. Shpitz, S. Gallinger, H. Nguyen, N.A. Hozumi, Transplantation 60 (1995) 179–184.
[64] G.W.J. Fleet, J.C. Son, Tetrahedron 44 (1988) 2637–2647.